Thermodynamic simulation of a multi-step externally fired gas turbine powered by biomass

A. Durante[a], G. Pena-Vergara[a], P.L. Curto-Risso[a], A. Medina[b], A. Calvo Hernández[b]

[a] *Departamento de Termodinámica Aplicada, Universidad de la República, Montevideo, Uruguay*

[b] *Department of Applied Physics, University of Salamanca, 37008 Salamanca, Spain*

Abstract

A thermodynamic model for a realistic Brayton cycle, working as an externally fired gas turbine fueled with biomass is presented. The use of an external combustion chamber, allows to burn *dirty fuels* to preheat pure air, which is the working fluid for the turbine. It also avoids direct contact of ashes with the turbine blades, resulting in a higher life cycle for the turbine. The model incorporates a high temperature heat exchanger and an arbitrary number of turbines and compressors, with the corresponding number of intercoolers and reheaters. It considers irreversibilities such as non-isentropic compressions and expansions, and pressure losses in heat input and release. The composition and temperature of the combustion gases, as well as the variable flow rate of air and combustion gases, are calculated for specific biomasses. The numerical model for a single stage configuration has been validated by comparing its predictions with the data sheets of two commercial turbines. Results are in good agreement. Curves on the dependence of thermal efficiency and power output with the overall pressure ratio will be shown for several plant configurations with variable number of compression/expansion stages. Also the influence of different types of biomasses and their moisture will be analyzed on parameters such as fuel consumption and exhaust gases temperature.

Keywords: Externally fired gas turbine, Open Brayton cycle, Solid biomass fuel, High temperature heat exchanger

PACS: 05.70.Ln, 07.20.Pe, 84.60.-h

Email addresses: adurante@fing.edu.uy (A. Durante), gabpena@fing.edu.uy (G. Pena-Vergara), pcurto@fing.edu.uy (P.L. Curto-Risso), amd385@usal.es (A. Medina), anca@usal.es (A. Calvo Hernández)

Nomenclature

Main model variables

$C_{\min}$: minimum heat capacity rate

C_r: heat capacity ratio

h_a: enthalpy of air

h_{fgH_2O}: vaporization enthalpy of water

h_g: enthalpy of exhaust gases

K: coefficient depending on HTHE construction materials and geometry

$\dot{m}_a$: air mass flow rate

$\dot{m}_f$: fuel mass flow rate

$\dot{m}_g$: exhaust gases mass flow rate

N_c: number of compressors

N_t: number of turbines

p: cycle pressures

P: power output

r_c: compressors pressure ratio

r_t: turbines pressure ratio

T_1: ambient temperature

T_2: temperature after each compression step

T_3: turbines inlet temperature

T_4: temperature at turbines outlet

T_{ad}: adiabatic flame temperature

$T_{e,1}$: exhaust temperature at the main combustion chamber

$T_{e,2}$: exhaust temperature at the intermediate reheaters

T_f: fuel temperature at inlet

x_i: mole fractions

Δp_H: pressure decay at heat input

Δp_L: pressure decay in the cold side of the cycle

ε: effectiveness of the HTHE

ε_c: compressors isentropic efficiency

ε_t: turbines isentropic efficiency

$\overline{\gamma}_{12}$: mean adiabatic coefficient in compression

$\overline{\gamma}_{34}$: mean adiabatic coefficient in expansion

ϕ_1: fuel-air equivalence ratio in the main combustion chamber

ϕ_2: fuel-air equivalence ratio in the reheaters

η: fuel conversion efficiency

Acronyms

d.b.: dry basis

EFGT: externally fired gas turbine

LHV: lower heating value

HTHE: high temperature heat exchanger

NTU: number of heat transfer units

UA: global exchange coefficient

1. Introduction

From the viewpoint of environmental concerns, sustainable development depends among other efforts on the reduction of greenhouse gases and the conservation of soil and water. These points require a rational use of fossil fuels and the utilization of renewable resources. Among human activities, energy production is one of the most intensively demanding natural resources. Simultaneously, it is by far the largest source of pollutant emissions. It could be stated with certainty that the future world energy supply will necessarily rely on a wide variety of energy resources, especially including renewable ones. Moreover, energy production should be adapted to the particular conditions and resources of countries or regions. Future technologies should combine high conversion efficiencies with low pollutant and greenhouse emissions.

Biomass is getting more attention because it is considered to have zero net CO_2 cycle [1, 2], as emitted CO_2 is consumed by the growing plants. Biomass is available in different forms, as it comes from forestry and agriculture, but also from animal and biodegradable urban wastes [3]. Because we are dealing with a natural resource spread out over geographically large areas, transportation and processing costs make it interesting for medium or small scale decentralized power plants. These scales are smaller than what is usually considered economically and thermodynamically advantageous for steam Rankine cycles [4]. Nevertheless, the use of gas turbines is advantageous due to their flexibility and scalability. Overall efficiencies of these plants usually is ranged between 15% for small plants to 30% for the largest ones. Anyway, these records are small compared for instance with standard combined cycle natural gas plants, but have the environmental benefits commented above.

Gas turbines are machines that require very clean gas for reliable operation. The externally fired gas turbine (EFGT) is a technology under development that tries to avoid the problem of burning dirty fuels to produce electricity through gas turbines. Since the working fluid through the turbine is separated from the combustion gases, the thermal power from combustion has to be transferred to the working fluid through a high temperature heat exchanger (HTHE). These heat exchangers are capable to operate at temperatures above 900°C. Ceramic materials are in the basis of their construction [5, 6]. EFGTs can be used in combined cycles such as Brayton (topping cycle) Rankine (bottoming) plants [7], heat and power (CHP) applications [8], and also hybridized with other renewable resources as thermosolar [9, 10]. Datta *et al.* [11], Vera *et al.* [12], Soltani *et al.* [2] have reported energy and exergy analysis of EFGT plants in the kW range including gasification units for distributed power generation. A recent work by M. Bdour *et al.* [13] gives a thorough overview on previous studies on biomass fueled EFGTs.

The aim of this work is to present and validate a thermodynamic model for an EFGT burning biomass. The model is stated in terms of the basic principles of thermodynamics and includes the main irreversibility sources existing in real installations. The model depends on a relatively low number of parameters, all of them with a clear physical interpretation. Key points in this kind of plants are considered in detail: the chemical reactions leading to the heat input in the cycle and the actual heat transfer in the HTHE. One of the main novelties of the model is that allows to consider an arbitrary number of compression steps with intermediate intercooling processes and also an arbitrary number of expansions with reheating between turbines. This strategy is devoted to search for plant configurations with increased overall efficiency, that the market is demanding. The model is validated in the case of a single stage configuration by comparing with real plants and then some results are obtained in relation to the influence of different types of biomass and their moisture on the plant performance. Also explicit curves on the dependence of power output and efficiency with the overall pressure ratio are shown. For instance, it will be demonstrated that power output of a plant with two compressors and one turbine is increased about 30% with respect to a single stage cycle without a large increasing of overall pressure ratio. Optimum pressure ratios to obtain maximum efficiency and power output are obtained for several plant configurations. Fuel consumption will be analyzed for different types of biomasses and also the influence of fuel moisture on parameters as fuel consumption and exhaust gases temperature will be surveyed.

2. Thermodynamic model

The model considers an arbitrary number of turbines, N_t, and compressors, N_c, with the corresponding $N_c - 1$ intercoolers and $N_t - 1$ intermediate burners complemented with a combustion chamber fueled by biomass and a ceramic HTHE (see Fig. 1 for a layout of the EFGT and Fig. 2 for the corresponding $T - S$ cycle).

The working fluid entering the first compressor is air at pressure P_1 and temperature T_1. It is compressed by N_c non-adiabatic compressors to pressure P_2 and temperature T_2, taken as identical for all of them. Between each pair of compressors, heat is extracted by an intercooler in order to decrease the temperature at each compressor inlet to T_1. After compression processes the air increases its temperature up to T_3 in the ceramic HTHE. The turbines inlet temperature T_3, is fixed according to constructive and metallurgical limits. Then, air is expanded by N_t non-adiabatic turbines up to pressure P_4 and temperature T_4. In the main combustion chamber the biomass is burned with clean air coming from the last turbine at temperature T_4. The equivalence ratio, ϕ_1, of this combustion is calculated so that the adiabatic flame temperature $T_{\rm ad}$ allows the air to reach T_3 at the exit of the HTHE. Exhaust gases leave the HTHE at a temperature $T_{e,1}$. After each expansion process, heat is supplied by the intermediate burners in order to increase the temperature at each turbine inlet to T_3. These burned gases are released to the ambient at temperature $T_{e,2}$. The combustion in the burners, which allows to heat the clean air from T_4 to T_3 in a separate circuit, uses air from the ambient at T_1. The equivalence ratio of this combustion, ϕ_2, is calculated so that the adiabatic flame temperature obtained matches with the one reached in the main combustion chamber. As a design criterion, a pinch point of 100 K on the exhaust gases temperature, $T_{e,2}$, is considered.

The thermodynamic cycle is based on previous results reported by some of us for a closed multistep and recuperative Brayton gas turbine suitable for an arbitrary number of turbines and compressors [14, 15] and the corresponding reheating and intercooling processes. Such model was latter applied to the thermodynamic modeling of a solar-driven and a hybrid solar gas-turbine power plant [16, 17, 18]. The present work adapts the model, for external combustion, explicitly considering the chemical reactions in the combustion of solid biomass. Next, we detail the main assumptions and definitions for each stage of the EFGT starting from the ideal Brayton-like cycle and introducing irreversibilities in real installations as pressure drops, non-ideal heat exchangers, and non-isentropic compressors and turbines.

2.1. Compression and expansion processes

In previous works it was demonstrated that in order to minimize power losses in the compression steps and maximize power output in the expansions, the pressure ratios of compressors should be identical, as well as, those for turbines [15, 19]. Under these conditions and assuming a mean isentropic coefficient for the air in each process, it is obtained that

$$T_2 = T_1 \left[1 + \left(\frac{a_c - 1}{\varepsilon_c} \right) \right] \tag{1}$$

where

$$a_c = \frac{T_{2s}}{T_1} = r_c^{\frac{\bar{\gamma}_{12}-1}{\bar{\gamma}_{12}}} \tag{2}$$

and $r_c = (p_2/p_1)^{1/N_c}$ is the pressure ratio of each compressor, $\bar{\gamma}_{12}$ the mean adiabatic coefficient in the $1 \to 2$ process, and ε_c the isentropic efficiency of each compressor defined as

$$\varepsilon_c = \frac{T_{2s} - T_1}{T_2 - T_1} \tag{3}$$

where T_{2s} represents the working fluid temperature after isentropic compression. Similarly, for the expansion we obtain:

$$T_4 = T_3 \left[1 - \varepsilon_t \left(1 - \frac{1}{a_t} \right) \right] \tag{4}$$

where

$$a_t = \frac{T_3}{T_{4s}} = r_t^{\frac{\bar{\gamma}_{34}-1}{\bar{\gamma}_{34}}} \tag{5}$$

and $r_t = (p_3/p_4)^{1/N_t}$ is the pressure ratio of each turbine, $\bar{\gamma}_{34}$ the mean air adiabatic coefficient in the $3 \to 4$ process, and ε_t represents the isentropic efficiency of each turbine defined as

$$\varepsilon_t = \frac{T_3 - T_4}{T_3 - T_{4s}}. \tag{6}$$

where T_{4s} represents the temperature at the turbines exit after an ideal isentropic expansion. Note in Fig.2 that the pressure ratio of each turbine and of each compressor are related by the pressure drops in the hot, Δp_H, and cold Δp_L sides of the heat exchangers as

$$\frac{p_3}{p_4} = \frac{p_2 - \Delta p_H}{p_1 + \Delta p_L} \tag{7}$$

These equations allow to obtain the temperature after the compression process, T_2, and after expansion, T_4, in terms of the pressure ratios, air temperature before the first compressor, T_1, and the turbine inlet temperature, T_3. The latter will be taken as an input design parameter in the plant model.

2.2. Combustion model

In order to solve the chemistry and the energetics of combustion, we assume a solid wet fuel with a particular chemical composition and humidity. For any kind of biomass, the considered chemical reaction can be written as [20]:

$$C_{a/12}H_{b/1}O_{c/16}N_{d/14} + f\, H_2O + \frac{\alpha_q}{\phi}(O_2 + 3.76\, N_2) \longrightarrow \\ \beta CO_2 + \gamma H_2O + \epsilon CO + \theta H_2 + \nu O_2 + \mu N_2 \quad (8)$$

where $C_{a/12}H_{b/1}O_{c/16}N_{d/14}$ represents one mole of dry fuel and a, b, c, and d is the amount of each element in mass percentage. The coefficient f represents the moles of water per mole of dry fuel, α_q the stoichiometric amount of O_2 in air, and ϕ the fuel-air equivalence ratio. It is noteworthy that this model does not take into account the possible presence of sulphur in the fuel. This is assumed because the presence of sulphur on biomass is usually not significant. Particularly, the biomasses considered in this work contain less than 0.1% sulphur. The combustion reaction is solved following the procedure described by Medina *et al.* [21].

2.3. Adiabatic flame temperature

It will be assumed that all the energy released from combustion is transferred to exhaust gases without losses, so $T_{\rm ad}$ is the temperature of exhaust gases assuming an adiabatic combustion. Thus, it can be calculated through an enthalpy balance in this way:

$$\dot{m}_f h_f(T_f) + \dot{m}_a h_a(T_{\rm air}) = \dot{m}_g h_g(T_{\rm ad}) \quad (9)$$

where $\dot{m}_f$, $\dot{m}_a$, and $\dot{m}_g$ are the mass flows of fuel, air, and burned gases respectively. The latter is obtained through a mass balance. It is assumed that the water in the fuel is in the liquid state at the fuel temperature, T_f. The specific enthalpy of air, h_a, is evaluated at the temperature, $T_{\rm air}$, that is T_4 for the main combustion chamber and T_1 for the intermediate burners.

The enthalpies of the fuel and burned gases are calculated as follows. Once the composition of burned gases is obtained by solving the chemistry of the combustion reaction, its enthalpy is given by:

$$h_g(T) = x_{CO_2} h_{CO_2}(T) + x_{H_2O} h_{H_2O}(T) + x_{O_2} h_{O_2}(T) + x_{N_2} h_{N_2}(T) + \\ x_{CO}\left[h_{CO}(T) + LHV_{CO}\right] + x_{H_2}\left[h_{H_2}(T) + LHV_{H_2}\right] + x_{\rm ash} c_{p,{\rm ash}}(T - T_{\rm ref}) \quad (10)$$

where x_i stands for the moles of each chemical component per mass flow rate of combustion gases, LHV_j is the lower heating value at reference temperature, T_{ref}, of specie j, and $c_{p,\text{ash}}$ is the specific heat of ashes, taken as temperature independent. The enthalpy of the fuel at T_f is given by:

$$h_f(T_f) = c_{p,f}(T_f - T_{\text{ref}}) + LHV_f - f\left[h_{fgH_2O} - c_{p,H_2O}(T_f - T_{\text{ref}})\right] \qquad (11)$$

where h_{fgH_2O} is the enthalpy of vaporization of water at the reference temperature and c_{p,H_2O} is liquid water specific heat. In numerical calculations it will be taken $T_f = T_{\text{ref}}$ in order to overcome the specific heat of biomasses. Once T_{ad} is calculated, the fuel ratio is estimated to meet the desired turbine inlet temperature, T_3.

2.4. HTHE effectiveness

The effectiveness of the HTHE is defined as:

$$\varepsilon = \frac{T_3 - T_2}{T_{\text{ad}} - T_2} \qquad (12)$$

This effectiveness depends, among other factors, on the mass flow rates, fluid properties and temperatures, and design criteria. An estimation calculated from the NTU method will be considered [22]. From this method, the effectiveness of any heat exchanger is a function depending on two parameters: $\varepsilon = \varepsilon(NTU, C_r)$ where NTU is the number of heat transfer units, $NTU = UA/C_{\min}$, UA is the global exchange coefficient, $C_{\min}$, the minimum heat capacity rate, and $C_r = C_{\min}/C_{\max}$, the heat capacity ratio. Considering a counter-flow scheme to model the HTHE [6, 22]:

$$\varepsilon = \frac{1 - e^{-NTU(1-C_r)}}{1 - C_r e^{-NTU(1-C_r)}} \qquad (13)$$

Taking the correlations of the Nusselt number for internal flow [22] and assuming that the thermodynamic properties of the working fluids do not considerably change for the temperature intervals of the cycle, the convection coefficient for air and exhaust gases only depends on the mass rates of air and exhaust gases. Thus, considering an internal flow for air and an external staggered tube bank for burned gases, NTU can be expressed as [22]:

$$NTU = \frac{K}{C_{\min}\left[\dot{m}_a^{-0.8} + \dot{m}_g^{-0.6}\right]} \qquad (14)$$

where the coefficient K depends on the design of the heat exchanger (geometry and construction materials) and the thermodynamic properties of the working fluids. In the validation section will be detailed the type of HTHE taken for numerical computations. Once, the HTHE has been characterized, the energy and mass balances of the main flux read as:

$$\dot{m}_{a,1}\left[h_a(T_3) - h_a(T_2)\right] = \dot{m}_{g,1}\left[h_{g,1}(T_{ad}) - h_{g,1}(T_{e,1})\right] \tag{15}$$

and $\dot{m}_{g,1} = \dot{m}_{a,1} + \dot{m}_{f,1}$ where $\dot{m}_{a,1}$ is the air mass flow rate through the compressors, $\dot{m}_{f,1}$ is the fuel rate in the main combustion chamber, and $\dot{m}_{g,1}$ the mass flow rate of exhaust gases going through the main HTHE. The subscript 1 was included in all flow rates to distinguish the main flow from those in the intermediate burners as will be shown next.

As depicted in Fig. 1, $N_t - 1$ intermediate burners ensure that the temperature at any turbine in the multi-step expansion is always the same, T_3. With this aim the fuel-ratio is fitted in order to increase the temperature from T_4 to T_3 after each partial expansion. Thus, the enthalpy balance for each intermediate burner reads as:

$$\dot{m}_{a,1}\left[h_a(T_3) - h_a(T_4)\right] = \dot{m}_{f,2}h_f(T_f) + \dot{m}_{a,2}h_a(T_1) - \dot{m}_{g,2}(T_{e,2}) \tag{16}$$

In this equation, the subscript 2 applies for fuel and air mass flow rates at the intermediate burners. $T_{e,2}$ is the temperature at the exhaust of these burners. It is noteworthy that the exhaust composition in this burners is different that in the main combustion chamber.

2.5. Power and efficiency

Once all the temperatures in the cycle were solved, the power output is calculated from:

$$P = N_t\dot{m}_{a,1}\left[h_a(T_3) - h_a(T_4)\right] - N_c\dot{m}_{a,1}\left[h_a(T_2) - h_a(T_1)\right] \tag{17}$$

The fuel conversion efficiency of the cycle gives the ratio between the actual power output and the available energy in the fuel flow rate [23], *i.e.*,

$$\eta = \frac{P}{\dot{m}_f\, LHV} \tag{18}$$

where $\dot{m}_f$ is the total fuel mass flow rate, that in the main combustion chamber and those in the intermediate burners, $\dot{m}_f = \dot{m}_{f,1} + \dot{m}_{f,2}$. Figure 3 is a flow chart showing how the submodels are linked in order to obtain the output records of the EFGT.

3. Model validation and numerical computations

It is difficult to find open and complete data sources for commercial EFGT turbines and still more complicated results for particular biomasses to compare with. We have applied the model developed in the previous sections to a particular one, AE-T100E micro turbine externally fired [24]. It is a single-shaft micro turbine with a centrifugal single stage compressor and a radial single stage turbine. Its performance records depend on the external heat source. With validation purposes, instead of using biomass, we obtained the parameters for that turbine fueled with methane. According to the manufacturer, the maximum turbine inlet temperature is 1123 K, the air mass flow rate 0.80 kg/s, the pressure ratio 4.5, and the electrical power output 85 kW. Our model predicts a power output of 86.3 kW that only differs 1.53% of the experimental one and an electrical efficiency of 23%, which is a reasonable value (the manufacturer gives an electrical efficiency of 30% for the same turbine with internal combustion and burning natural gas). For the calculations, the coefficient K in Eq. (14) was taken to match the maximum effectiveness of a ceramic high temperature heat exchanger of the type developed in the work by de Mello and Monteiro [6].

In order to complete the validation of the model, we have compared its predictions with a directly fired commercial gas turbine, for which detailed data are available. This is the one-shaft Turbec T100 micro turbine fueled with natural gas [25]. Table 1 contains some parameters taken from the turbine data sheet and implemented in the model, and Table 2 the comparison of measured and model predicted data. As shown in Table 2, in spite of the differences in combustion (direct or external) model predictions are in good agreement with measured data.

Eucalyptus wood is taken as the primary fuel for the numerical calculations. Composition details in dry basis (*d.b.*) and lower heating value are collected in Table 3 [20]. Other biomasses (eucalyptus leaves and bark, rice husk, and pine wood) are additionally considered in order to analyze the influence of fuel compositions and different heating values (see below). Ashes heat capacities were estimated by using the Neumann-Kropp rule [22] and their elemental composition [20]. It was found that ashes heat capacity for any type of biomass is between 0.74 and 0.80 kJ/(K kg), thus an effective value of 0.77 kJ/(K kg) was used in computations for all samples.

3.1. Influence of pressure ratio

The pressure ratio is one of the basic design parameters influencing Brayton cycle performance. The EFGT plant performance was computed as a function of pressure ratio, r_c, for different configurations. Following Horlock's notation [26]: CT, single step plant with one compressor and one turbine; CICT, two compressors, one intercooler, and one turbine; CTBT, one compressor and two turbines with an intermediate burner; and CICTBT, two compressors with intercooling, and two turbines with reheating. Pressure ratio was varied from 2 to 16 and eucalyptus wood was taken as fuel with 25% moisture on dry basis. The air mass flow is set to 1.0 kg/s, the ambient temperature to 300 K and the turbine inlet temperature to 1273 K. All other parameters, as compressors and turbines isentropic efficiencies are the same that for the Turbec T100 turbine, Table 1.

Power output is depicted in Fig. 4. For the simplest one-step configuration, CT, power output presents a maximum at a relatively small value of the pressure ratio and afterwards it decays when pressure ratio increases. As indicated in Table 4 maximum power is found at about $r_{c,\max P} = 5.5$, and leads to $P_{\max} = 136$ kW. As seen in Fig. 4, the inclusion of another compressor with the corresponding intercooler, configuration CICT is able to increase power output about 39% at a higher global pressure ratio, that now is $r_{c,\max P} = 9.5$. The effect of adding a turbine with an intermediate reheater, CTBT, with respect to the basic CT layout provokes a similar effect in power output. It increases about 29% at the expense to take a pressure ratio about 10. In both configurations, the decrease of power output when r_c is over its maximum value is very slow, which means that with pressure ratios above approximately 8 power output yield is good and quite insensitive to r_c. Oppositely, to take advantage of the most complex layout, that with two compressors and two turbines, CICTBT, it is imperative to consider much higher values of pressure ratio. Just as a guide, the model predicts that this configuration is capable to increase P over the simplest layout at $r_c = 10$, about 84%.

Fuel conversion efficiency (see Fig. 5) presents a maximum in terms of the pressure ratio at not too high values of r_c for all checked configurations except for CICTBT, where the maximum is over 16. For each case, the pressure ratio leading to maximum efficiency, $r_{\max,\eta}$, is smaller than that corresponding to maximum power output, $r_{c,\max P}$ (see table 4). Maximum efficiency is found for the configuration CICT, 25%, closely followed by CT, 23%. In the case of more than one turbine, efficiency is penalized by the heat released by intermediate burners. Soltani *et al.* [1] have found a value of about 3.8 for the pressure ratio leading to maximum thermal efficiency for a CT plant with biomass gasification (taking as biomass wood with 20% moisture) and turbine inlet temperature of 1400 K. This value is very close to the predicted by our model, in spite that no gasification process is considered. In the case reported by Soltani *et al.* [1] maximum thermal efficiency was found to be 32% for the Brayton cycle. When combining it with a bottoming Rankine efficiency increases to approximately 47%. Similarly, Kautz and Hansen [9] found a pressure ratio leading to maximum electrical efficiency at 2.9 for a recuperated CT configuration with turbine parameters from Turbec T100. In this case methane was taken as fuel and the turbine inlet temperature was set to 1223 K. The electric efficiency was raised from 16% to 30% by incorporating recuperation.

An alternative way to analyze the optimum range of parameters for the design of the system is by plotting the parametric power-efficiency curves. In the case shown in Fig. 6 the pressure ratio was taken as a parametric variable. The pressure ratio increases clockwise in the curves. The optimum range of r_c is that corresponding to the interval between $r_{c,\max\eta}$ (that always is smaller than $r_{c,\max P}$) and $r_{c,\max P}$. In the curves this is the interval between the highest point (maximum efficiency) and maximum power output (rightmost point). Other configurations outside that region are not convenient in the sense that there exist other pressure ratios giving simultaneously more power and more efficiency. So, the optimal pressure ratio for plant design (at least in which respect to the optimization of efficiency and power output) should be a compromise between those ones. In the figure the curves corresponding to the configurations CT and CTBT are the narrowest. This means that the interval of pressure ratios leading to maximum efficiency or power is relatively narrow in these configurations and so, it is possible to attain reasonable good values of both output records simultaneously. This is reflected in Table 4, where it can be seen that this interval is between $r_c = 3.5$ (maximum efficiency) and $r_c = 5.5$ (maximum power output) for CT and between $r_c = 6.0$ (maximum efficiency) and $r_c = 9.5$ (maximum power output) for CTBT. On the other side, the maximum power output for the configuration CICTBT is reached for quite large values of r_c, so the corresponding power efficiency curves is open (taking as plotting the interval for r_c the same that for the other configurations). In any case the efficiency of the configurations with more than one turbine is small because the heat released by the intermediate burners is not efficiently profited in the cycle itself.

The temperature of exhaust gases after the HTHE, $T_{e,1}$ (see Fig. 1), is plotted in Fig. 7 against the pressure ratio. Exhaust temperature has a strong dependence on r_c. In the model developed this is associated to the coupling between Eqs. (1) and (15). In the figure it is seen that there are two levels of exhaust temperatures. A higher one for the simplest configuration, CT, and that one with two turbines and an intermediate burner. And a lower one for the configurations with two compressors and intercooling between them, CICT and CICTBT. Roughly speaking, difference between these two levels is around 100 K for $r_c = 5$. For all ayouts, exhaust temperatures are high, so it is feasible and advisable from the viewpoint of overall efficiency to couple the EFGT to a combined heat and power system or directly to include a bottoming steam Rankine cycle [27, 28].

3.2. Analysis of different biomasses

Numerical computations were performed for different biomasses, always considering an air flow mass of 1.0 kg/s, $T_1 = 300$ K, $T_3 = 1173$ K, and 25% moisture on d.b. Pressure ratio was set to 4.5. Biomasses chemical composition is contained in Table 3 and fuel consumptions and efficiencies in Table 5. Eucalyptus wood was taken as reference biomass. From the table it is apparent that there are two levels of fuel consumption for eucalyptus wood, those corresponding to layouts with one turbine and those with two stage expansion. In the former fuel consumption is between 0.033 and 0.035 kg/s and in the later about twice due to the consumption on the intermediate burner. This affects efficiency, that for the configurations CT and CICT is between 0.22 and 0.25 and for CTBT and CICTBT between 0.12 and 0.14.

Comparing eucalyptus wood with other biomasses, eucalyptus leaves and pine wood result in reduced consumption for any plant layout (about 5.5% for eucalyptus leaves and 3.2% for pine wood) and so increased efficiency (between 0.42 and 0.84 for eucalyptus leaves and between 0.18 and 0.48 for pine wood). Due to the lower heating values of eucalyptus bark and rice husk, fuel consumption increase for these biomasses (about 17% for eucalyptus bark and about 25% for rice husk). In consequence, efficiency decreases between 1.24% and 3.36%. Although they are not shown in the table other two types of biomasses were investigated, eucalyptus branches and eucalyptus tips. In both cases LHV is quite similar to eucalyptus leaves and so, fuel consumption and efficiencies are similar to eucalyptus wood.

3.3. Influence of fuel moisture

The influence of fuel moisture was analyzed in the case of eucalyptus wood biomass. All parameters were taken as in the preceding section except T_3 that was taken as 1273 K. Cycle net power output is independent of fuel moisture if ambient and turbine inlet temperatures, and the air mass flow rates are fixed. On the contrary, fuel consumption and efficiency are sensitive to moisture. With increasing moisture a larger fuel mass rate is required to keep the turbine inlet temperature at the desired value, because less useful energy is contained in the fuel per unit mass. Figure 8 represents the behavior of fuel consumption in terms of moisture as a percentage on dry basis. Fuel consumption is of course larger for plant configurations with more than one turbine. For all configurations the shape of the increase of consumption with moisture is similar. It is not completely linear, but parabolic and to have a rough idea the increase amounts about 35 % in the whole interval, from 0 to 100% moisture. This increase in fuel consumption is reflected in efficiency as depicted in Fig. 9. The decrease in efficiency is almost linear for all layouts and has a higher slope for the cases CT and CICT. In the latter, the drop in the whole interval is very substantial, about 37 %. Al-Attab *et al.* [3] comment that 10% efficiency can be achieved by biomass pre-drying with fuel moisture content from 50% to 80%. From our calculations, it is predicted an increase between 8% and 14%, depending on the configuration, from 50% to 0% moisture.

Adiabatic flame temperature in the main combustion chamber and the exhaust gases after the HTHE are plotted in Fig. 10. Provided that fuel consumption increases with the fuel moisture, the gas mass flow increases in order to keep constant the turbine inlet temperature. This makes larger the heat exchange at the HTHE and in consequence the adiabatic flame temperature in the main combustion chamber slightly decreases with increasing fuel moisture (see Fig. 10(a)). However, exhaust gases temperature appreciably increases with moisture (see Fig. 10(b)). For instance, for the configuration CICT, from about 893 K for 0% moisture to 953 K for 100%. This represents an increase of about 7%. This also influences the decline on efficiency curves in terms of moisture in the fuel.

4. Summary and conclusions

An original model for a plant producing electricity by means of a biomass externally fired gas turbine scheme has been developed, implemented, and validated. From the thermodynamic viewpoint, the model incorporates the possibility to analyze several plant configurations. An arbitrary number of compressors with intermediate intercooling and also an arbitrary number of turbines with in-between reheaters is considered. The model accounts for the main thermal losses in these kind of installations: non-ideal compressors and turbines and pressure losses in heat absorption and heat release. It is remarkable that the model includes detailed chemistry of combustion for several types of biomass and their moisture. The fuel-air ratios, both in the main combustion chamber as well as in the intermediate reheaters are explicitly considered. Furthermore, specific calculations for the HTHE, assumed ceramic heat exchanger are included. So, the dependence of variable temperature ranges and working fluid mass rates are incorporated in the calculation of heat transfer and so, plant output records. The model allows to analyze all the most significant parameters in plant design and operation.

A validation process has been followed, by comparing model predictions with a commercial mono-step EFGT fueled with methane. Deviations among model predictions and the real turbine are small. Also, a qualitative validation by comparing with a directly fired gas turbine was performed. In all cases comparisons were satisfactory.

With respect to the analysis of model predictions the work was focused on the power output scale of about one hundred kW and on two particular points: on one hand, on the effects of pressure ratios on fuel conversion efficiency and power output, and on the other hand, on the influence of moisture in the fuel. Efficiency and power output curves when plotted against pressure ratio display a maximum. The curve of efficiency for the configuration CICT is, for any value of pressure ratio, above all other configurations checked. Pressure ratio leading to maximum efficiency is always lower than that corresponding to maximum power output. The incorporation of a second compressor over a basic one step configuration allows an important power output increase (about 30% for a pressure ratio giving maximum power) and an slight increase on maximum efficiency (that increases from 23% to 24.5%). The configurations with more than one turbine are not convenient except if some kind of recuperation mechanism is considered, because of the heat released by intermediate reheaters to the ambient. Even in the more efficient configurations it would be possible to use a bottoming Rankine cycle to take advantage of the high temperatures of exhaust. The moisture of biomass has a clear influence on fuel consumption, efficiency, and exhaust gases temperature. For all these variables explicit curves were shown in all the moisture interval and for all the plant configurations analyzed. For instance a decrease of moisture from 50% d.b. to 0% will lead to increase efficiency between 8% and 14%, depending on the particular plant layout. Open for future work along this line is the search of plant schemes including recuperation from the main combustion chamber exhaust and in the case of multiple turbines from intermediate reheaters. Also, to enhance overall plant efficiency by coupling heat release to a bottoming cycle by means of a heat recovery steam generator.

Acknowledgements

A. Durante, G. Pena-Vergara, and P.L. Curto-Risso acknowledge support from Agencia Nacional de Investigación e Innovación (ANII, Uruguay), grant FSE-1-2014-1-102079 and from the SNI program that supports their research. The authors from University of Salamanca are grateful for financial support from MINECO of Spain, Grant ENE2013-40644-R and University of Salamanca.

[1] S. Soltani, S. M. S. Mahmoudi, M. Yari, M. A. Rosen, Thermodynamic analyses of an externally fired gas turbine combined cycle integrated with a biomass gasification plant, Ener. Conv. Manage. 70 (2013) 107–115.

[2] S. Soltani, M. Yari, S. M. S. Mahmoudi, T. Morosuk, M. A. Rosen, Advanced exergy analysis applied to an externally-fired combined-cycle power plant integrated with a biomass gasification unit, Energy 59 (2013) 775–780.

[3] K. Al-Attab, Z. Zainal, Externally fired gas turbine technology, Appl. Energ. 138 (2015) 474–487.

[4] B. Elmegaard, E. B. Qvale, G. Carapelli, P. de Faveri Tron, Open-cycle indirectly fired gas turbine for wet biomass fuels, in: Proceedings of Efficiency, Cost, Optimization, Simulation, and Environmental Impact of Energy Systems (ECOS 2001), International Center for Applied Thermodynamics, Istanbul, 2001, pp. 361–367.

[5] B. Sunden, High temperature heat exchangers (HTHE), in: Proceedings of the Fifth International Conference on Enhanced, Compact and Ultra-Compact Heat Exchangers: Science, Engineering and Technology, Hoboken, NJ, USA, 2005.

[6] P. E. B. de Mello, D. B. Monteiro, Thermodynamic study of an EFGT (Externally Fired Gas-Turbine) cycle with one detailed model for the ceramic heat exchanger, Energy 45 (2012) 497–502.

[7] S. M. Camporeale, A. M. Pantaleo, P. D. Ciliberti, B. Fortunato, Cycle configuration analysis and techno-economic sensitivity of biomass externally fired gas turbine with bottoming ORC, Ener. Conv. Manage. 105 (2015) 1239–1250.

[8] I. W. Eames, K. Evans, S. Pickering, A comparative study of open and closed heat-engines for small scale CHP applications, Energies 9 (2016) 130.

[9] M. Kautz, U. Hansen, The externally fired gas turbine (EFGT-cycle) for decentralized use of biomass, Appl. Energ. 84 (2007) 795–805.

[10] Q. Liu, Z. Bai, X. Wang, J. Lei, H. Jin, Investigation of thermodynamic performances for two solar-biomass hybrid combined cycle power generation systems, Ener. Conv. Manage. 122 (2016) 252–262.

[11] A. Datta, R. Ganguly, L. Sarkar, Energy and exergy analyses of an externally fired gas turbine (EFGT) cycle with biomass gasifier for distributed power generation, Energy 35 (2010) 341–350.

[12] D. Vera, F. Jurado, B. de Mena, G. Schories, Comparison between externally fired gas turbine and gasifier-gas turbine system for the olive oil industry, Energy 36 (2011) 6720–6730.

[13] M. Bdour, M. Al-Addous, M. Nelles, A. Ortwein, Determination of optimized parameters of the flexible operation of a biomass-fueled, microscale externally fired gas turbine (EFGT), Energies 9 (2016) 856.

[14] A. Calvo Hernández, A. Medina, J. M. M. Roco, Power and efficiency in a regenerative gas turbine, J. Phys. D: Appl. Phys. 28 (1995) 2020–23.

[15] A. Calvo Hernández, J. M. M. Roco, A. Medina, Power and efficiency in a regenerative gas-turbine with multiple reheating and intercooling stages, J. Phys. D: Appl. Phys. 29 (1996) 1462–68.

[16] S. Sánchez-Orgaz, A. Medina, A. Calvo Hernández, Thermodynamic model and optimization of a multi-step irreversible Brayton cycle, Energ. Convers. Manage. 51 (2010) 2134–43.

[17] S. Sánchez-Orgaz, A. Medina, A. Calvo Hernández, Recuperative solar-driven multi-step gas turbine power plants, Energ. Convers. Manage. 67 (2013) 171–178.

[18] D. Olivenza-León, A. Medina, A. Calvo Hernández, Thermodynamic modeling of a hybrid solar gas-turbine power plant, Energ. Convers. Manage. 93 (2015) 435–447.

[19] B. D. Joshi, Thermodynamic work for n-step isothermal processes involving an ideal gas, J. Chem. Educ. 63 (1986) 24–25.

[20] L. Barbosa, E. Silva, E. Olivares, Biomassa para energia, Editora Unicamp, 2008.

[21] A. Medina, P. L. Curto-Risso, A. Calvo Hernández, L. Guzmán-Vargas, F. Angulo-Brown, A. K. Sen, Quasi-dimensional simulation of spark ignition engines, Springer, 2014, Appendix E.

[22] T. Bergman, A. Lavine, F. Incropera, D. Dewitt, Fundamentals of heat and mass transfer, 7th Edition, Wiley, 2012.

[23] J. Heywood, Internal Combustion Engine Fundamentals, McGraw-Hill, 1988.

[24] [link].
URL `http://www.atetsrl.it/Content/Atet/Images/Partner/Ansaldo/allegato%20(3).`

[25] [link].
URL `http://people.unica.it/danielecocco/files/2012/07/Microturbina_T100_Detail`

[26] J. Horlock, Advanced Gas Turbine Cycles, Pergamon, Oxford, 2003.

[27] R. Carapellucci, A unified approach to assess performance of different techniques for recovering exhaust heat from gas turbines, Ener. Conv. Manage. 50 (2016) 1218–1226.

[28] Y. Cao, Y. Gao, Y. Zheng, Y. Dai, Optimum design and thermodynamic analysis of a gas turbine and ORC combined cycle with recuperators, Ener. Conv. Manage. 116 (2016) 32–41.

Fuel type	Methane
Gas turbine inlet temperature	1123 K
Air mass flow	0.7833 kg/s
Pressure ratio	4.5
Compressor isentropic efficiency	0.768
Turbine isentropic efficiency	0.826

Table 1: Parameters from the data sheet of the turbine Turbec T100 [25]. They are taken as input parameters in our model.

	Turbec T100	Model predictions	Relative deviations (%)
Net electric power output	100 kW	98.82 kW	1.18
Thermal power input	333 kW	360.68 kW	8.31
Turbine power	282 kW	281.34 kW	0.23
Compressor power	159 kW	158.37 kW	0.40
Net electric efficiency	30%	27.6 %	8.00
Compressor outlet temp.	487 K	487.4 K	0.18
Fuel flow rate (methane)	0.0067 kg/s	0.007188 kg /s	7.28
Exhaust flow rate	0.79 kg/s	0.7905 kg/s	0.063

Table 2: Comparison of the measured parameters for the Turbec T100 micro turbine [25] with those computed from our model.

Biomass	C (%)	H (%)	O (%)	N (%)	Ash (%)	LHV (kJ/kg)
Eucalyptus wood	49.0	5.9	44.0	0.3	0.1	18129
Eucalyptus leaves	54.9	5.9	35.8	1.0	2.4	19100
Eucalyptus bark	44.7	5.4	41.8	0.2	4.9	15800
Rice husk	41.0	5.9	35.9	0.4	18.9	14800
Pine wood	49.3	6.0	44.4	<0.01	0.3	18681

Table 3: Elemental compositions (*d.b.*) and lower heating values [20] for the considered biomasses.

Configuration	$r_{c,\max\eta}$	$\eta_{\max}$	$r_{c,\max P}$	$P_{\max}$ (kW)
CT	3.5	0.23	5.5	136
CTBT	6.0	0.13	9.5	189
CICT	4.5	0.25	10.0	176
CICTBT	16.0	0.17	>16	>266

Table 4: Maximum fuel conversion efficiency, $\eta_{\max}$, and maximum power, $P_{\max}$, for several plant configurations. The corresponding values of the pressure ratio are also shown: $r_{c,\max\eta}$ and $r_{c,\max P}$ respectively.

	Fuel cons. (kg/s)	Relative differences (%)			
Configuration	Eucalyptus wood	Eucal. leaves	Eucal. bark	Rice husk	Pine wood
CT	0.033	-5.70	17.17	26.87	-3.28
CTBT	0.074	-5.51	16.11	24.98	-3.22
CICT	0.035	-5.72	17.19	26.84	-3.27
CICTBT	0.072	-5.53	16.30	25.20	-3.14
	Efficiency	Relative differences (%)			
Configuration	Eucalyptus wood	Eucal. leaves	Eucal. bark	Rice husk	Pine wood
CT	0.22	0.84	-2.00	-3.32	0.48
CTBT	0.12	0.47	-1.24	-2.05	0.29
CICT	0.25	0.72	-1.98	-3.36	0.44
CICTBT	0.14	0.42	-1.31	-2.21	0.18

Table 5: Fuel consumption rate and efficiency for different biomasses. Relative differences are calculated with respect to eucalyptus wood.

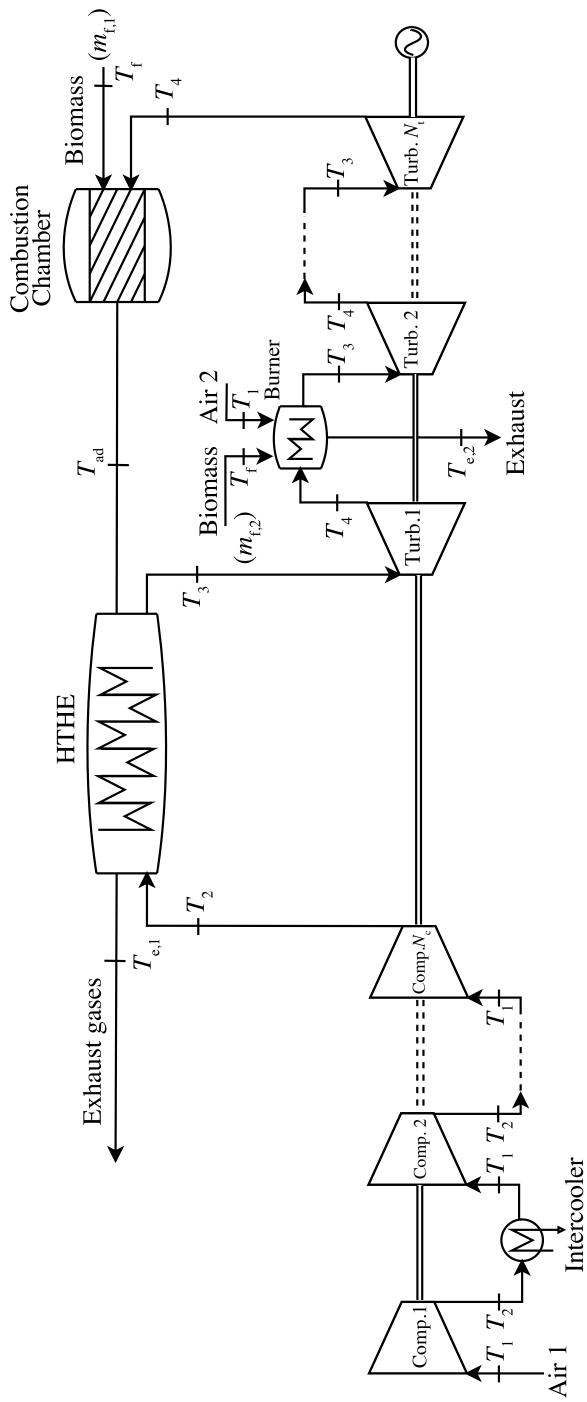

Figure 1: Scheme of the multi-step EFGT plant considered.

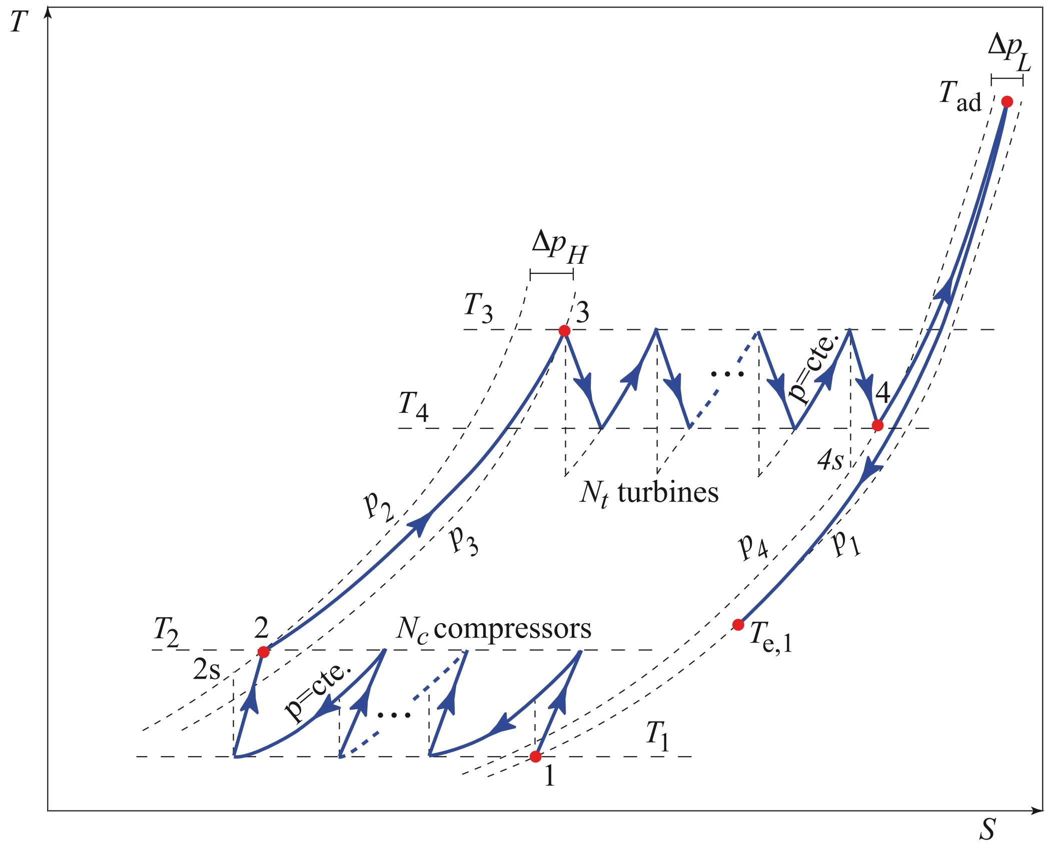

Figure 2: Temperature-entropy diagram for the Brayton cycle. Pressure losses in heat input and release, as well as, non-isentropic compression and expansion processes are considered.

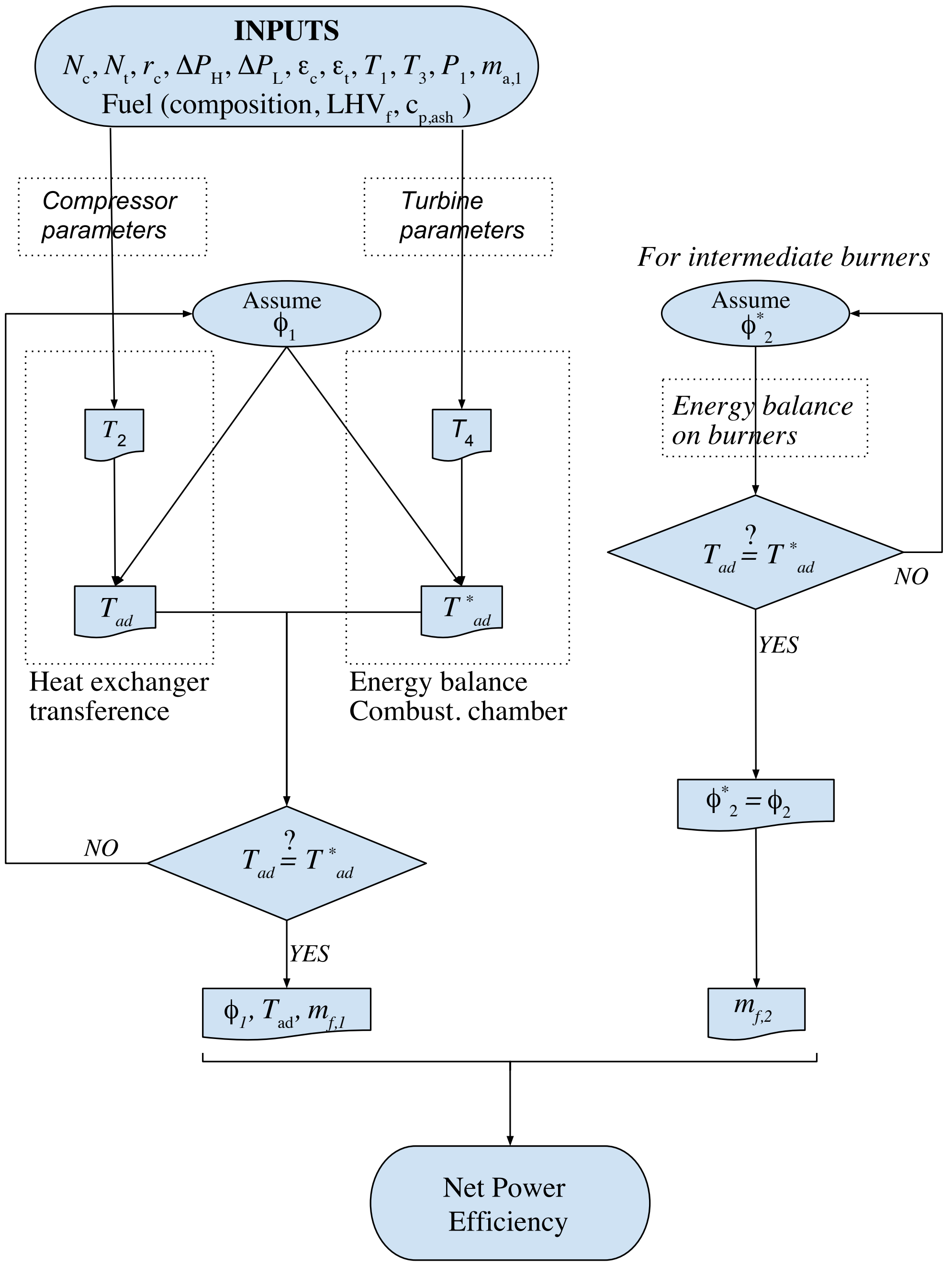

Figure 3: Flow chart of the iterative procedure followed to compute the power output and thermal efficiency of the EFGT plant.

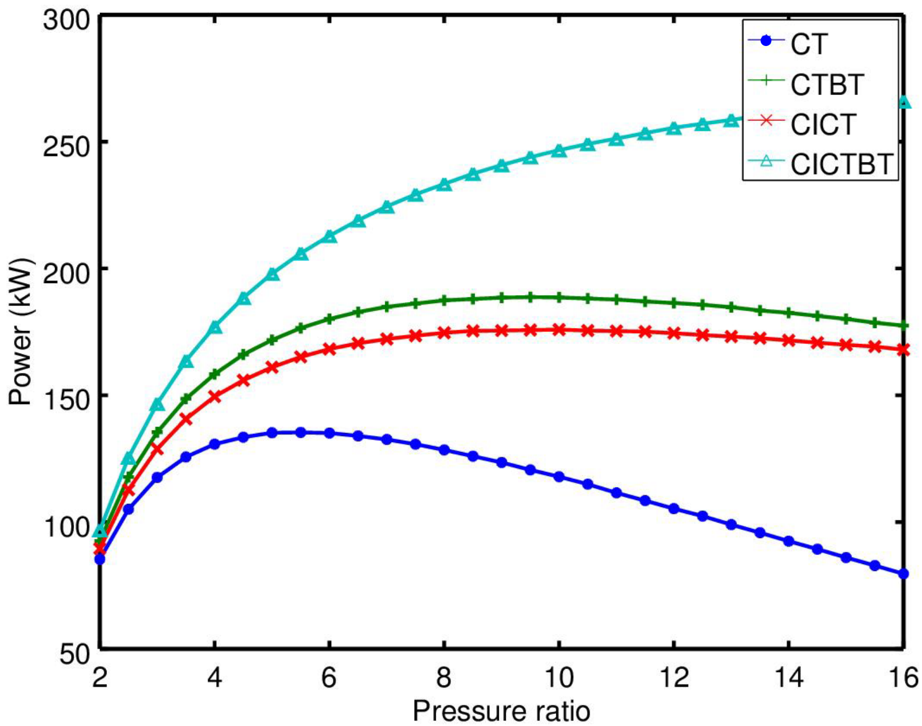

Figure 4: Evolution of power output with the pressure ratio for four different plant layouts as explained in the main text.

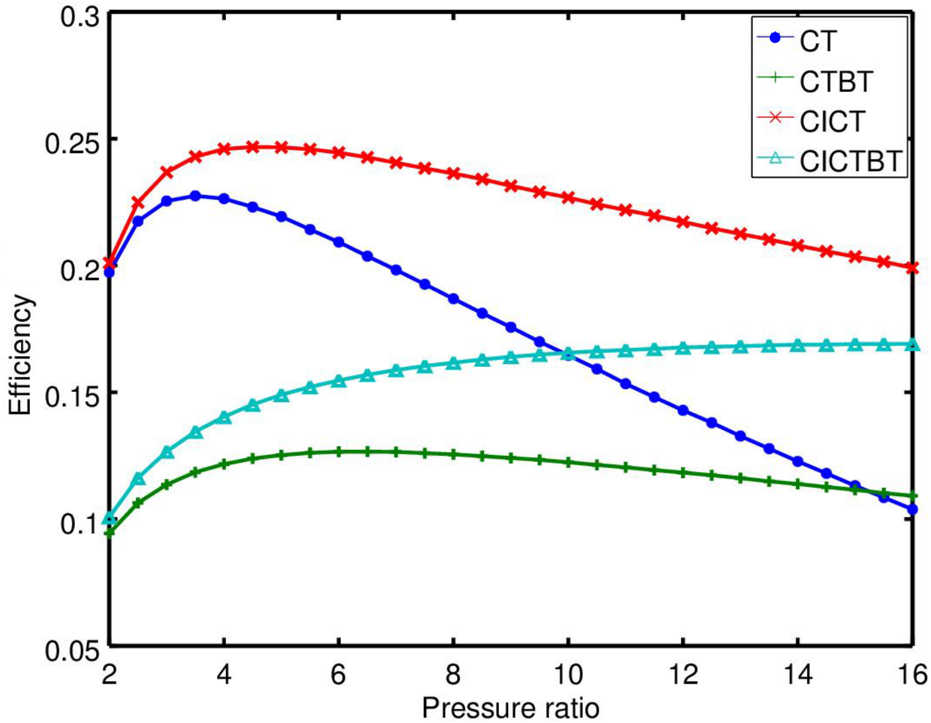

Figure 5: Evolution of fuel conversion efficiency with the pressure ratio for the considered plant configurations.

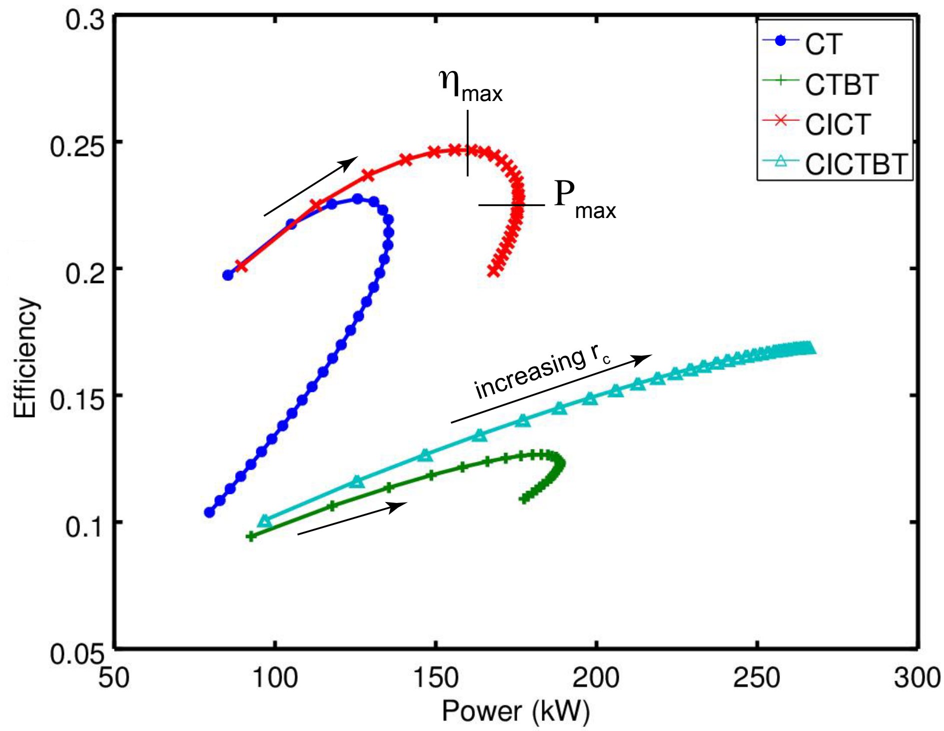

Figure 6: Implicit power-efficiency curves obtained by eliminating r_c between the curves $\eta(r_c)$ and $P(r_c)$. The arrows indicate increasing values of r_c. For clarity (see text) in the particular case of the configuration CICT the maximum efficiency and maximum power points are shown. The region in between should be considered as the optimum one for plant design (considering as objective functions power and efficiency and the pressure ratio as optimizing parameter).

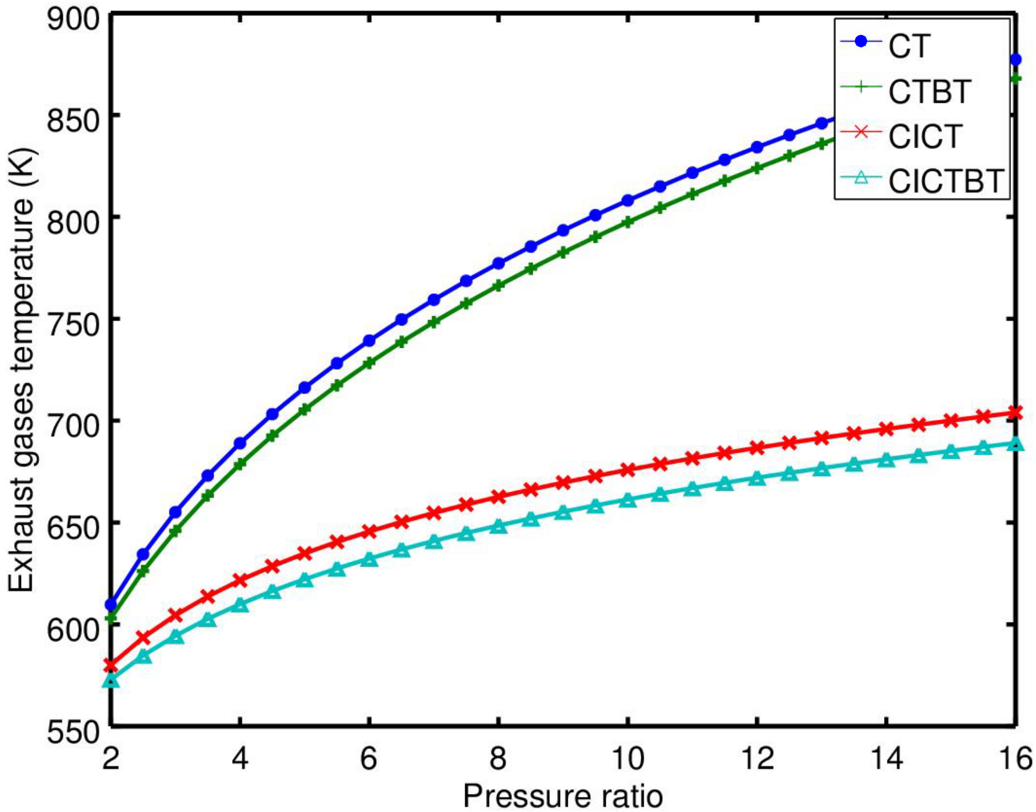

Figure 7: Temperature of exhaust gases after the HTHE, $T_{e,1}$ (see Fig. 1), for a single stage configuration, CT, and for several multi step layouts.

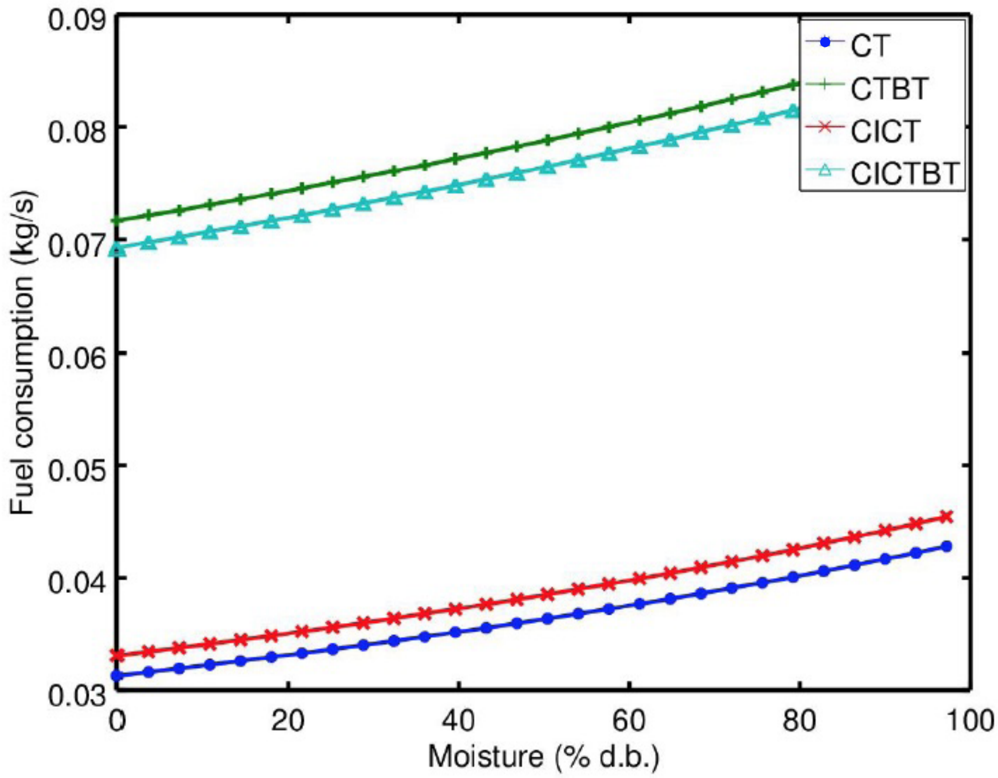

Figure 8: Dependence of fuel consumption with fuel moisture in the case of burning eucalyptus wood. Pressure ratio was fixed at 4.5 and the plant layout includes two compressors and one turbine, CICT configuration. The air mass flow in the combustion chamber was set to 1.0 kg/s, the ambient temperature at 300 K, and the turbine inlet temperature at 1273 K.

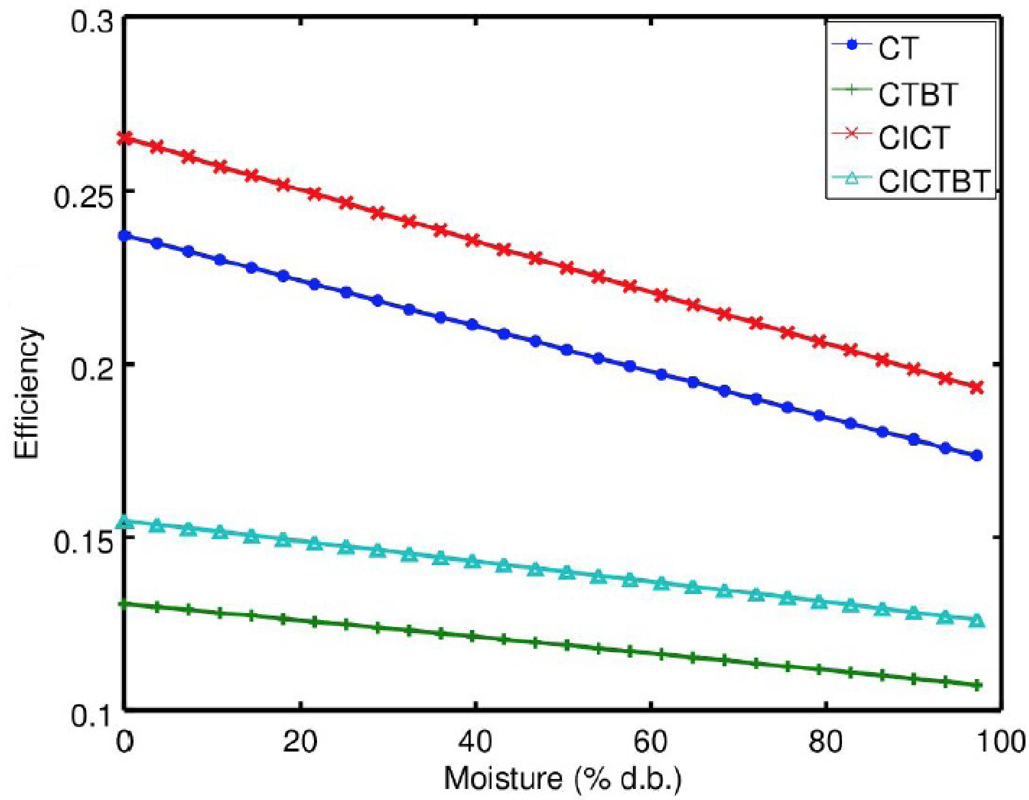

Figure 9: Influence of fuel moisture on the fuel conversion efficiency. Data are the same that in Fig. 8.

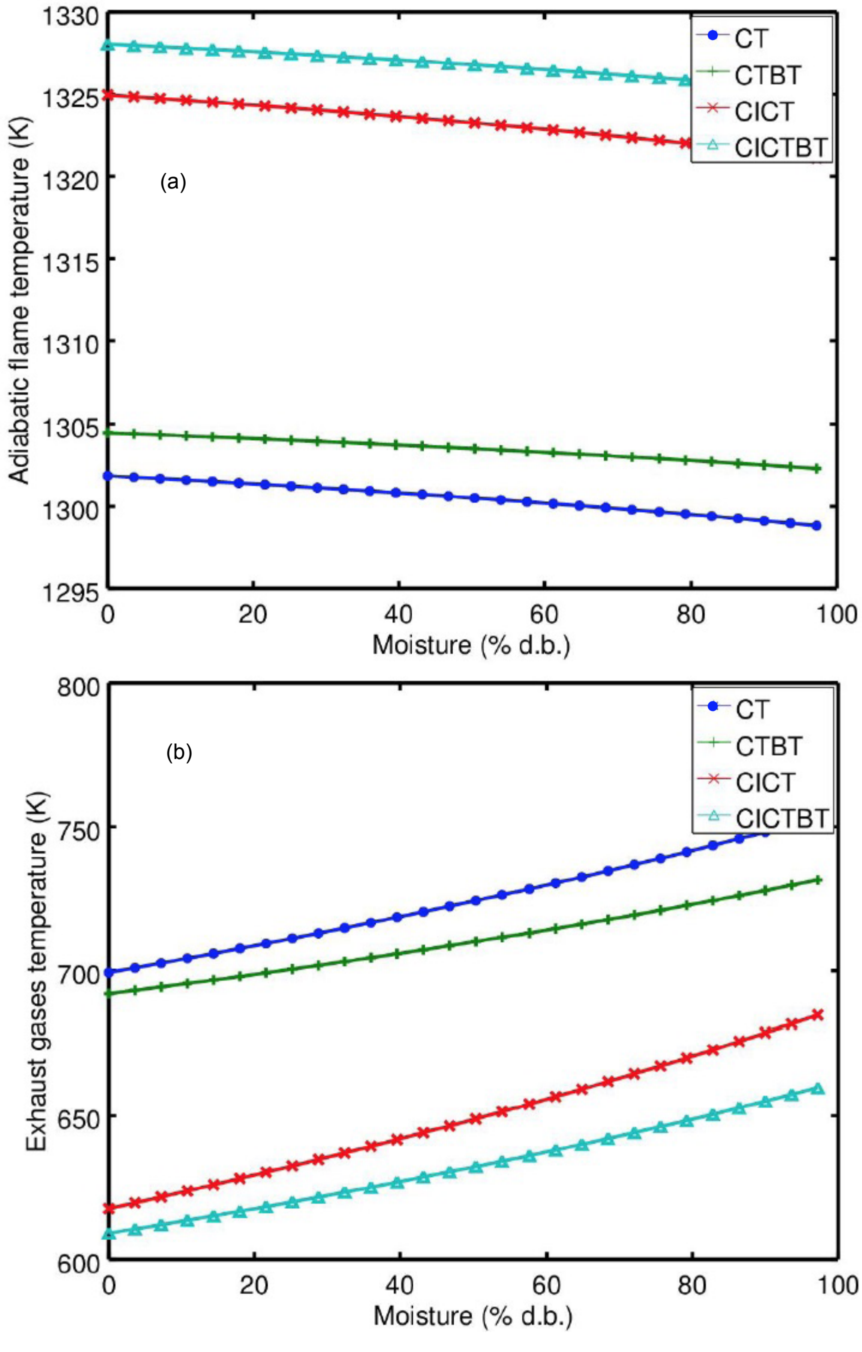

Figure 10: (a) Influence of fuel moisture on adiabatic flame temperature, $T_{\rm ad}$, and (b) on exhaust gases temperature, $T_{e,1}$. Data are the same that in Fig. 8.